CHAPTER 5. MODEL SELECTION AND COMPUTATIONAL PROCEDURES

5.1 INTRODUCTION

In experimental studies of heterogeneously catalised reactions, it must always be confirmed that the investigation is concerned with catalytic kinetics and not with interactions between the kinetics and transport phenomena, thermodynamic constraints or homogeneous gas phase reactions. The intrusion of temperature and concentration gradients can lead to severe deviations in a catalyst's performance completely disguising the true kinetics of the reaction. To ensure that the experimental results are suitable for kinetic evaluation, both temperature and concentration gradients within the individual catalyst particle (Intra-particle gradients), from the external surface of the particle and the fluid adjacent to them (Inter-phase gradients) and between the local fluid regions or catalyst particles (Inter-particle gradients) must be eliminated. If the various gradients are not eliminated during the experimental study, then a two-dimensional reactor model (Smith 1988:544) in combination with heterogeneous models to describe both mass and heat transfer phenomena in and around the catalyst particle have to be used. Using a variety of criteria, the extent of deviations from ideal plug flow and the presence of temperature and concentration gradients in both the pilot plant and the bench scale reactor systems were quantified. Where possible the conclusions reached during the theoretical investigation were confirmed experimentally. The results of this investigation are presented here in Chapter 5 and the details of the various theoretical procedures used in Appendix 4. Also included here are the details of the computational procedure used to quantify the ability of the various mechanistic models developed in predicting the performance of the system. Motivation for considering the various models, as well as the results obtained, are presented in Chapter 6. The robustness of the final model developed, using the data generated in the bench scale reactor system, was confirmed by using it to predict the performance of the pilot plant reactor system. These results are given in Chapter 6.

For details of the bench scale reactor system used during the kinetic study of the n-butene skeletal isomerisation reaction, see Chapter 3. Details of the operating and data

manipulation procedures used, as well as of the analytical techniques, were discussed in Chapter 3 and Appendices 1 and 2. The results obtained while investigating the effects of the operating conditions and feed composition on the performance of the catalyst, were discussed previously in Chapter 4. A comprehensive review of the relevant literature is presented in Chapter 2.

5.2 SIGNIFICANCE OF AXIAL AND RADIAL TRANSPORT LIMITATIONS

The flow in single phase packed bed reactors may deviate from ideal plug flow due to variations in the axial as well as the radial direction. The significance of these deviations for both the pilot plant and the bench scale reactor system were investigated. If this deviation is substantial, then the one-dimensional plug flow reactor models can not be used and a two-dimensional mass and energy conservation model as shown in Appendix 4, Section A4.2 is required.

5.2.1 SIGNIFICANCE OF RADIAL MASS TRANSFER LIMITATIONS

The flow in a packed bed reactor may deviate from ideal plug flow due to variations in the axial velocity, in the radial direction. This radial variation in the velocities leads to a residence time distribution. It has been reported by Smith (1981:557) that this deviation from ideal plug flow is not significant if the ratio of the tube (d_T) to particle (d_p) diameter, i.e., (d_T/d_P) is greater then thirty. Whitaker (1969:14) on the other hand suggested that a tube to particle diameter ratio in excess of only 10 is required to ensure that radial transport effects may be neglected. However, even when applying continuum models either pseudo-homogeneous or heterogeneous to fixed bed chemical reactors, Vortmeyer and Winter (1984:1431) showed that a lower limit exists beyond which the models are no longer valid. They set this limit at a tube to particle diameter ratio of $d_T/d_P \geq 4$. In this study, spherical catalyst particles with a diameter of between 1.2 mm and 2.0 mm and weighted average diameter of 1.5 mm, were used. Using the extreme particle diameters, this translates for the pilot plant with a tube diameter d_T = 25.4 mm, to a tube to particle ratio

of between 21.2 and 12.7 and for the bench reactor with a tube diameter of d_T = 13.1 mm, to a tube to particle ratio of between 10.9 and 6.6. As in the latter case, the ratio of the tube to particle diameter is less than 10, variations in the axial velocity in the radial direction may exist. However, as mass transport effects are negligible compared to heat transport effects (Mears, 1971:544) the significance of mass transport effects can be confirmed by evaluating the importance of radial heat transport limitations. In this study the criterion developed by Mears (1971:545), the details of which are given in Appendix 4 and as discussed in Section 5.2.2, was used to confirm that even in the latter case, the significance of radial mass transfer limitations were not significant.

5.2.2 SIGNIFICANCE OF RADIAL HEAT TRANSFER LIMITATIONS

Deviations from ideal plug flow, i.e., variations in the axial velocity in the radial direction that lead to residence time distributions may also occur under extreme conditions as during highly exothermic reactions (Froment and Bischoff, 1979:451). To quantify the degree of deviation, the criterion proposed by Mears (1971:545) was evaluated. If the criteria is met, then a deviation from ideal plug flow due to radial heat transport effects of less than 5 % may be assumed. However, the absolute validity of this approach is questioned due to the multitude of relationships required to calculate the various parameters involved (See Appendix 4) and due to the results presented by other workers. Keyser (1996:A13) found, while studying the highly exothermic Fischer Tropsch reaction ($-\Delta H$ = 165 kJ·mol CO^{-1}) using catalyst with a diameter of 3 mm in a fixed bed tubular reactor with internal diameter of 20.93 mm, i.e., dimensions similar to the pilot plant reactor, and tube to particle ratio d_T/d_p of 6.9, that a one-dimensional model was more than adequate in describing the system. In Keyser (1996:A13) the criteria proposed by Mears (1971:545) was violated by more than a factor of four. Never the less, in this study, the criteria was applied and satisfied by the bench scale reactor system, the reactor system used to generate the data required for the kinetic investigation. For the pilot plant, a deviation from ideal plug flow due to radial heat transport effects of only 6 % was indicated. Radial heat transfer limitations were therefore considered to be negligible in both cases (See also Appendix 4, Table A4.5). This conclusion was further confirmed upon calculating the radial temperature

gradient using a two-dimensional homogeneous model. This gradient was found to be less than 1°C. (See Appendix 4, Section A4.3.16 for details). Hence, as radial heat transport effects are not significant it may also be concluded that radial mass transport effects, which are negligible compared to heat transport effects, (Mears, 1971:544), are not significant enough to justify the use of a two-dimensional reactor model.

5.2.3 SIGNIFICANCE OF AXIAL MASS TRANSFER LIMITATIONS

The flow in packed bed reactors may also deviate from ideal plug flow due to axial mixing effects. For isothermal operations back mixing or axial dispersion is considered to be negligible if the aspect ratio of the bed height (L) to particle diameter (d_P) is greater than 50, while in the case of non-isothermal operation a minimum value of 300 is required (Carberry, 1981:76). Westerterp et al. (1993:212) on the other hand concluded that back mixing does not take place if the bed height to particle diameter ratio is greater than 10. In the pilot plant, containing 50 g of catalyst, the bed height (L = 151 mm) to average particle diameter (d_P = 1.5 mm) ratio was 101. For the bench scale system, using the same catalyst particles (d_P = 1.5 mm) between 7.35 g (bed height = 84 mm) and 13 g (bed height = 148 mm) of catalyst were loaded corresponding to a bed heights to particle diameter ratio of L/d_p = 56 and L/d_p = 99 respectively. As in all cases the values calculated exceed the criteria proposed by Westerterp et al. (1993:212) axial mass transport effects were considered negligible. Alternatively, when the rate is monotonically decreasing in the bed, the critical position where the importance of axial mixing has to be assessed is at the bed inlet. An appropriate criterion to check for deviations from ideal plug was developed by Young and Finlayson (1973) as reported by Froment and Bischoff (1990:448). As is shown in Appendix 4, Table A4.6, this criterion was met for both the pilot plant and the bench scale reactor systems. Hence, deviation from ideal plug flow due to axial mixing was not considered significant enough to require the use of a two-dimensional reactor model.

5.2.4 SIGNIFICANCE OF AXIAL HEAT TRANSFER LIMITATIONS

When the reaction rate is maximum at some intermediate position in the catalyst bed because of a hot spot for example, the importance of axial mixing has to be assessed at this point. However, when the rate is monotonically decreasing in the bed, as during isothermal operation, the critical position where the importance of axial mixing has to be assessed is at the bed inlet. An appropriate criterion to check for deviations from ideal plug due to heat transfer limitations was developed by Young and Finlayson (1973) as reported by Froment and Bischoff (1990:448). As is shown in Appendix 4, Table A4.6, this criteria was met for both the pilot plant and the bench scale reactor system. Hence, deviation from ideal plug flow due to axial heat transport limitations was also not significant enough to require the use of a two-dimensional reactor model.

5.3 FLUID / PARTICLE HEAT AND MASS TRANSFER RESISTANCES

To enable the development of an intrinsic kinetic equation it has to be confirmed that both inter- and intra-particle heat and mass transfer resistances are negligible, i.e., that the temperature and the partial pressure of the reactants and products in the bulk of the fluid are equal to those on the surface and at the centre of the catalyst particle. Details of the criterion used, while determining whether heat and mass transfer effects were significant enough to warren the use of heterogeneous models, are given below.

5.3.1 INTER-PARTICLE HEAT TRANSFER LIMITATIONS

For vapour phase systems, the greater part of the resistance to heat transfer is often in the boundary layer or film around the catalyst particle, rather than within. This happens because the effective thermal conductivity of the solid is usually much larger than the conductivity of the gas phase. In the case of a highly exothermic reaction the particle temperature can become considerably higher than the bulk stream temperature. A criterion for detecting the onset of a heat transport limitation was developed by Mears

(1971:128) using the perturbation approach and applied to both the pilot plant and bench scale reactor systems. It was found that in both cases the observed rate deviated by less than 5 % from the surface rate due to inter-particle heat transport limitations. See also Appendix 4, Section A4.9 and Table A4.7 for further detail.

5.3.2 INTER-PARTICLE MASS TRANSFER LIMITATIONS

If the rate of mass transfer across the external stagnant film surrounding the catalyst particle is comparable to the surface reaction rate, then the supply of reactant to the catalyst particle as well as the reaction rate contribute to the observed global rate. As during kinetic investigations the intrinsic kinetics are sought, the validity of the assumption that the bulk and surface concentrations are equal and that the rate of reactant supply to the catalyst via diffusion across the stagnant film is in excess of the rate of reactant consumption via chemical reaction, has to be confirmed. Starting from the bulk reaction rate, the reaction rate at the adjacent surface may be approximated using a Taylor expansion (Kreyszig, 1979:694, Everson et al.,1996:238). Using this approach, the appropriate criteria was developed, as discussed in detail in Appendix 4, Section A4.10. It was found that for both the pilot plant and the bench scale reactor system the significance of inter-particle mass transfer resistances were not significant. (See also Table A4.7 in Appendix 4 for further detail).

The conclusion, that film diffusion was not rate limiting, was also investigated experimentally. Using the procedure as proposed by Koros and Nowak (1967) and as presented by Froment and Bischoff (1990:173), as a guide line, the effect of changing the linear velocity while maintaining a constant residence time, on the performance of the catalyst was determined. In this way the thickness of the stagnant film of fluid surrounding the catalyst particles was altered and the degree to which diffusion of the reactants across this film was rate limiting, established. In this study the superficial linear velocity was varied over a wide range of between 40 m/h and 600 m/h at constant residence times of 0.5 s, 1.3 s, 1.5 s and 2.5 s, by loading a suitable amount of catalyst and adjusting the flow rates accordingly. The results are shown in Figures 5.1 to 5.4 and Tables 5.1 to 5.4. From

this investigation it may be concluded that above a linear velocity of 120 m/h the n-butene skeletal isomerisation performance of the catalyst was independent of the linear velocity, i.e., that film diffusion limitations were absent. In the subsequent kinetic study the linear velocity was held above 200 m/h in all cases to ensure that film diffusion was negligible.

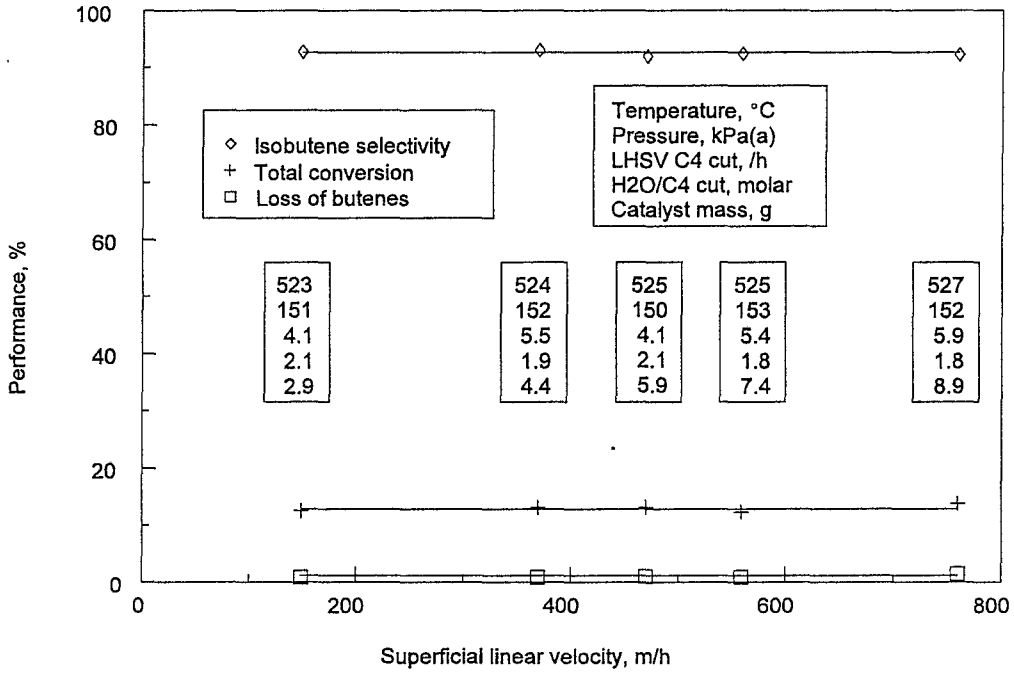

Figure 5.1 : Effect of the linear velocity on the n-butene skeletal isomerisation performance at a constant residence time of 0.5 s

TABLE 5.1 : CATALYST PERFORMANCE - RESIDENCE TIME = 0.5 S

Linear Velocity, m/h	149	369	470	559	760
n-Butene Conversion, %	12.5	13.1	13.1	12.3	13.8
Isobutene Yield, %	11.6	12.2	12.1	11.4	12.3
Loss of Butenes, %	0.9	0.9	1.1	0.9	1.5
Isobutene Selectivity, %	92.8	93.1	92.0	92.4	92.2
Cracking selectivity, %	3.9	4.1	3.7	2.9	3.8
Hydrogenation Selectivity, %	0.3	0.2	1.3	0.9	0.7
Oligomerisation Selectivity, %	3.0	2.6	3.1	3.8	3.3

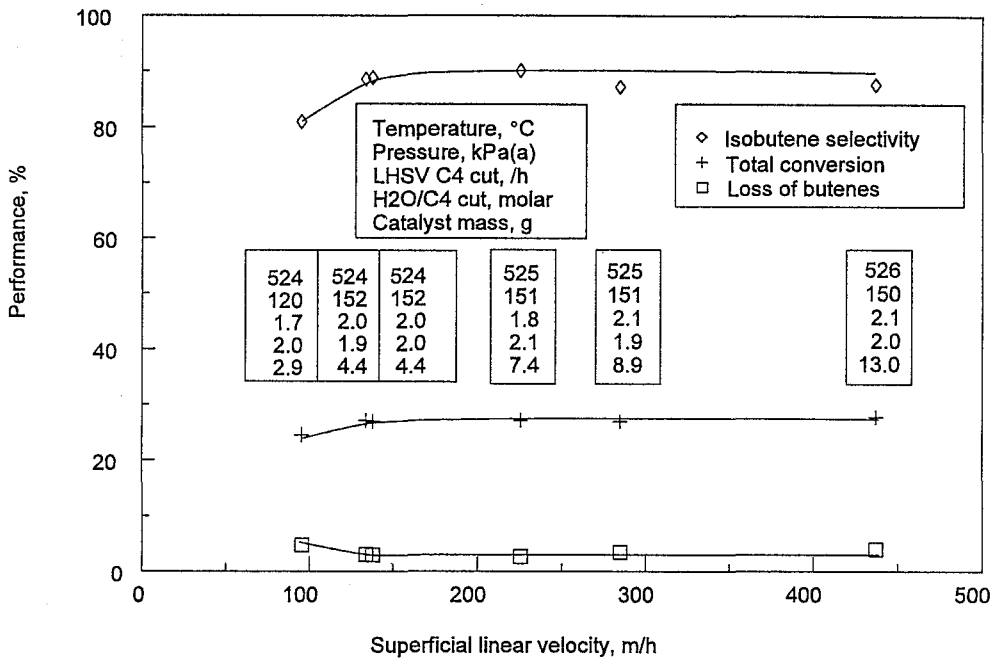

Figure 5.2 : Effect of the linear velocity on the n-butene skeletal isomerisation performance at a constant residence time of 1.3 s

TABLE 5.2 : CATALYST PERFORMANCE - RESIDENCE TIME = 1.3 S

Linear Velocity, m/h	95.3	134	138	226	285	437
n-Butene Conversion, %	24.5	27.2	26.9	27.1	26.9	27.7
Isobutene Yield, %	19.8	24.1	23.9	24.4	23.5	24.3
Loss of Butenes, %	4.7	3.1	3.0	2.7	3.5	4.0
Isobutene Selectivity, %	80.9	88.6	88.8	90.1	87.2	87.6
Cracking selectivity, %	11.1	6.1	6.6	5.5	6.0	5.6
Hydrogenation Selectivity, %	2.4	0.8	0.4	0.8	1.7	0.8
Oligomerisation Selectivity, %	5.5	0.8	0.4	0.8	1.7	0.8

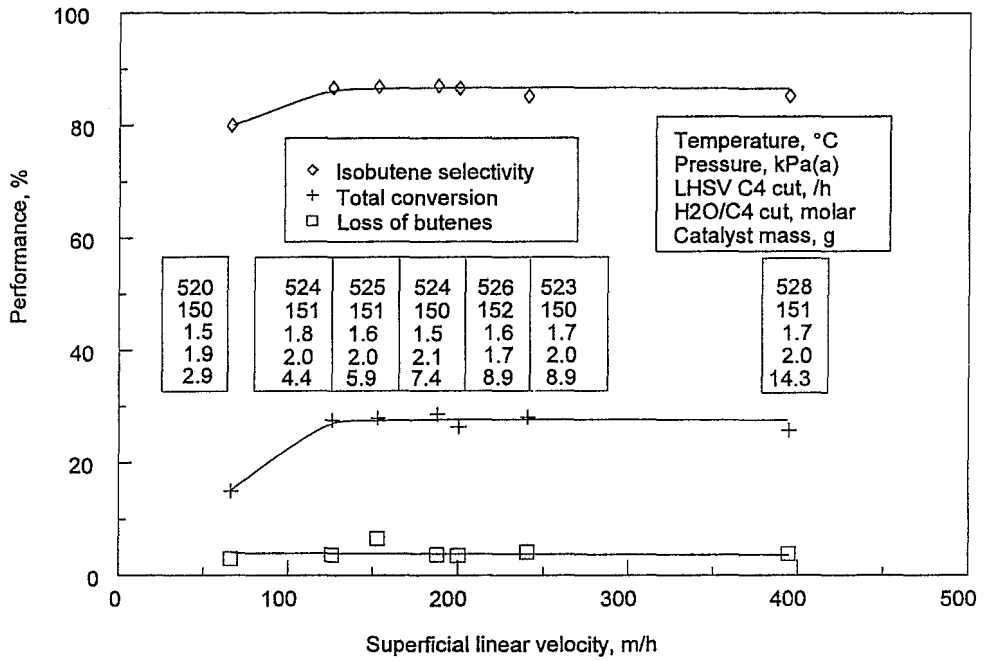

Figure 5.3 : Effect of the linear velocity on the n-butene skeletal isomerisation performance at a constant residence time of 1.5 s

TABLE 5.3 : CATALYST PERFORMANCE - RESIDENCE TIME = 1.5 S

Linear Velocity, m/h	66	126	153	188	200	241	395
n-Butene Conversion, %	15.0	27.6	27.9	28.6	26.4	28.1	25.7
Isobutene Yield, %	12.0	23.9	24.2	24.9	22.8	23.9	21.9
Loss of Butenes, %	3.0	3.7	6.6	3.7	3.6	4.2	3.8
Isobutene Selectivity, %	80.0	86.7	86.8	87.0	86.5	85.1	85.2
Cracking Selectivity, %	10.7	6.9	6.6	6.4	6.0	7.3	4.7
Hydrogenation Selectivity, %	2.1	0.5	0.8	1.0	1.0	1.3	0.8
Oligomerisation Selectivity, %	7.2	5.9	5.7	5.6	6.4	6.3	9.3

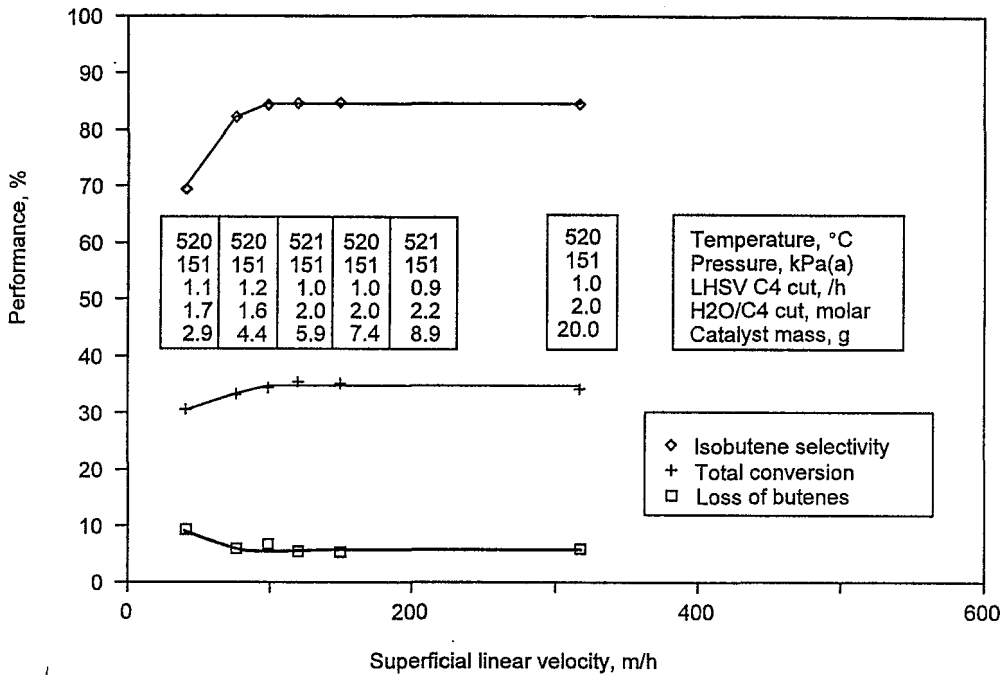

Figure 5.4 : Effect of the linear velocity on the n-butene skeletal isomerisation performance at a constant residence time of 2.5 s

TABLE 5.4 : CATALYST PERFORMANCE - RESIDENCE TIME = 2.5 S

Linear Velocity, m/h	41	75	76	118	145	152	289
n-Butene Conversion, %	29.9	32.4	33.3	35.5	35.3	34.4	33.5
Isobutene Yield, %	20.4	27.4	27.4	30.0	29.9	27.7	28.0
Loss of Butenes, %	9.5	5.0	5.9	5.4	5.4	6.7	5.4
Isobutene Selectivity, %	68.3	84.5	82.2	84.7	84.8	80.4	83.7
Cracking Selectivity, %	17.9	7.0	8.9	7.5	9.0	11.2	6.3
Hydrogenation Selectivity, %	5.6	1.2	1.7	1.9	1.2	2.0	1.3
Oligomerisation Selectivity, %	8.2	7.3	7.2	6.0	4.9	6.4	8.7

5.3.3 INTRA-PARTICLE HEAT TRANSFER LIMITATIONS

It may be assumed that heat transfer through the film around the catalyst particle will become limiting before heat transfer through the catalyst particle itself becomes limiting (Mears,1971:128, 1971:542). As it was already confirmed that film heat transfer limitations were not significant, it was to be expected that intra-particle heat transfer limitations would also not be significant. This assumption was confirmed, See Table A4.8 in Appendix 4, by using two criteria proposed by Mears (1971:128, 1971:542), as discussed in detail in Appendix 4, Section A4.11

5.3.4 INTRA-PARTICLE MASS TRANSFER LIMITATIONS

The presence of intra-particle diffusion resistance to mass transfer can be quantified by the relationship between the effectiveness factor and the Thiele modulus (Froment and Bischoff, 1990:159). Using the procedures presented by Aris (1957) as reported by Froment and Bischoff (1990:160) the Thiele modulus was calculated and the effectiveness factor evaluated. Alternatively, the effectiveness factor may also be calculated from diffusion considerations using the procedure presented by (Froment and Bischoff, 1990:158). Using these procedures, as discussed in detail in Appendix A4, Section A4.12 and Table A4.8, it was found that for both the pilot plant and the bench scale reactor system, intra-particle mass transfer limitations were also not significant. To experimentally confirm the conclusion that pore diffusion was not rate limiting, the catalyst was ground, using a mortar and pestle, sieved into different size fractions and the n-butene skeletal isomerisation performance of these fractions evaluated. In this way the effect of exposing sites located within the catalyst particle, and so the extent to which pore diffusion may be limiting, determined. In this study, fractions with particles between 0.25 to 0.5 mm, 0.5 to 1.0 mm, 1.0 to 1.19 mm and 1.19 to 2.0 mm were evaluated. It may be seen from Figure 5.5 and Table 5.5, the performance of the catalyst remained constant irrespective of the particle size fraction used, i.e., intra-particle mass transfer limitations are not significant. Hence, the standard commercial size catalyst particles, with an average diameter of 1.5 mm was used in all subsequent experiments.

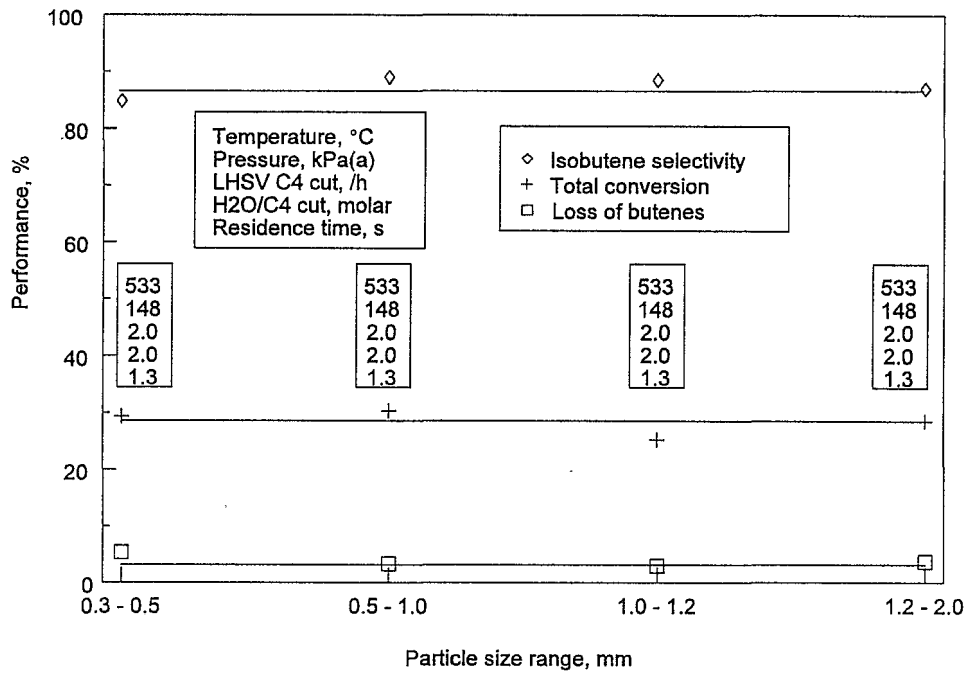

Figure 5.5 : Catalyst n-butene skeletal isomerisation performance vs catalyst size fraction

TABLE 5.5 : EFFECT OF PARTICLE SIZE ON CATALYST PERFORMANCE

Size Fraction, mm	0.3 - 0.5	0.5 - 1.0	1.0 - 1.2	1.2 - 2.0
Residence Time, s	1.5	1.5	1.5	1.6
Linear Velocity, m/h	205	205	205	195
n-Butene Conversion, %	29.4	30.3	25.3	28.6
Isobutene Yield, %	24.0	27.0	22.4	24.9
Loss of Butenes, %	5.3	3.3	3.0	3.7
Isobutene Selectivity, %	84.8	89.0	88.6	87.0
Cracking Selectivity, %	8.0	5.7	6.6	6.4
Hydrogenation Selectivity, %	1.5	1.0	0.8	1.0
Oligomerisation Selectivity, %	5.7	4.3	4.1	5.6

5.4 REACTOR MODEL SIMPLIFICATION

The reactor model can also be simplified if the linear velocity is independent of the axial location. The linear velocity may be effected by temperature gradients, pressure gradients and changes in the total molar / volumetric flow rate. The contribution of each of these on the linear velocity was examined.

5.4.1 ADIABATIC TEMPERATURE POTENTIAL

In the absence of losses, i.e., if the reactor is operated adiabatically, the heat generated during an exothermic reaction has to be removed via the effluent stream. Hence, the temperature at the outlet will always be higher than the temperature at the inlet. At the base case operating conditions, the potential adiabatic temperature rise was calculated to be 9.3 K. For details of the relationship used (Westerterp et al., 1993:267) see Appendix 4, Section A4.7. However, the heat losses from the pilot plant and the bench scale reactor system far outweighed the heat generated. Heat had to be added to both of these systems continuously, via the electric heating element strapped to the outside of the reactors. In this way the desired isothermal temperature profile could be maintained at all times. For a detail description of the reactor systems see also Chapter 3.

5.4.2 AXIAL TEMPERATURE PROFILE

An example of the temperatures recorded over the entire length of both the bench scale and pilot plant reactor systems are shown in Chapter 3. It was found that isothermal operation in the bench scale reactor system was achieved over a total length of 15 cm allowing for a maximum of 13 g of catalyst to be loaded. In the case of the pilot plant, the temperature profile recorded showed that isothermal behaviour through out the 150 mm catalyst bed and beyond was achieved. From routine checks of the temperature profile in both the pilot plant and the bench scale reactor system during the various experimental investigations performed and theoretical radial temperature profile calculated using a two-

dimensional reactor model (See Appendix 4, Section A4.3.16 for details) it was concluded that in both systems isothermal behaviour in the radial and axial direction was maintained.

5.4.4 AXIAL PRESSURE PROFILE

During the experimental work via direct measurement of the reactor inlet and outlet pressures to within an accuracy of 1 kPa(a), it was found that the pressure drop across the reactor system was less than 1 kPa(a). Using the procedure developed by Ergun (1952:89), see Appendix 4, Section A4.6, the pressure drop across both the pilot plant and bench scale reactor systems were calculated. At the base case conditions, the pressure drop across the pilot plant was calculated to be 0.11 kPa(a) and across the bench scale reactor system 0.03 kPa(a) when 7.35 g and 0.11 kPa(a) when 13 g of catalyst was loaded. As the pressure drop was found to be negligible using both a theoretical and experimental approach, it was concluded that the reactor system was operated isobarically.

5.4.5 AXIAL MOLAR FLOW PROFILE

Neither during the bond and skeletal isomerisation of the butenes, nor during the formation of hydrogenated / dehydrogenated products (n-butane, isobutane and butadiene) does the total number of moles change. Similarly, as the light (C_1 to C_3) and heavy (C_5^+) by-products are assumed to be formed via a butene dimerisation and cracking mechanism, no change in the total number of moles takes place. Combining this with the fact that at the base case conditions the butenes only constituted 33.3 mole % of the total feed, the balance being water, and that the conversion of the n-butenes to the various by-products was less than 3.5 mass % at the base case conditions, implies that the total molar flow rate does not change as a function of the axial position. The small quantity of coke formed, less than 0.2 mass % of the total hydrocarbon fed to the pilot plant reactor during a 32 h on line period, was not considered to be significant.

5.5 THERMODYNAMIC CONSTRAINTS

It is of course not possible to investigate the kinetics of a system in which the composition of the products are independent of the operating conditions, i.e., at thermodynamic equilibrium. During the kinetic investigation presented in Chapter 6, only results for which the isobutene to n-butene ratio in the product gas was less then 75 % of the theoretical value predicted from thermodynamics, were used.

The data presented previously while testing for inter- particle mass transfer was used to determine whether the relative ratios of the butenes in the product gas were at equilibrium, as predicted from thermodynamics. The calculated ratios, as a function of the residence time, as well as the theoretical values as predicted from thermodynamics, are shown in Figure 5.6. (See also Chapter 2, Section 2.3.6 for a detailed discussion of the effects of the temperature on the thermodynamic equilibrium ratio of the four isomers of butene.) Examining the partial pressure ratios of the linear butenes in the product gas, it may be seen from Figure 5.6 that these were, irrespective of the residence time used, equal to the ratio predicted from thermodynamics. Thus, as was concluded previously in Chapter 4, Section 4.2, the linear butene may be treated as a single pseudo-component, namely n-butene. It was further reported in Section 4.2 that at residence times in excess of 2.2 s, at 530°C, the four isomers of butene were in equilibrium. As may be seen from Figure 5.6, in this case the isobutene to n-butene partial pressure ratio in the product gas approaches the ratio predicted from thermodynamics as the residence time was increased but did not achieve this value. This difference may easily be understood as the feed used during the current study was pure 1-butene while that used previously contained on average 8.5 % isobutene. Hence, in the present study the catalyst has to work that much harder to achieve the same conversion, i.e. degree of approach to the thermodynamic equilibrium.

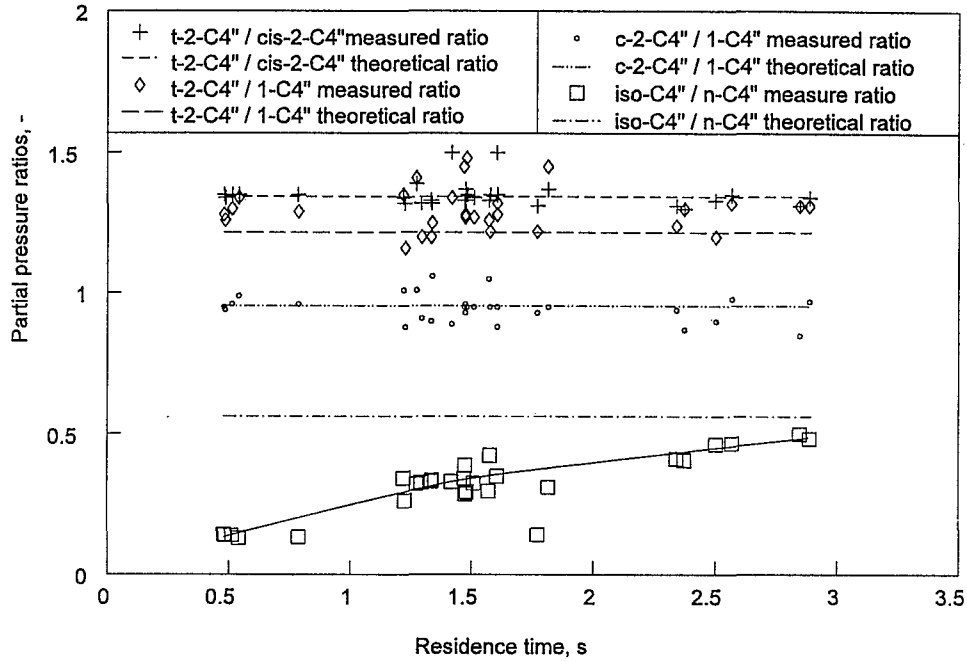

Figure 5.6 : Effect of the residence time on the butene partial pressure ratios in the product gas

5.6 BY-PRODUCT FORMATION

At the conditions employed, 1-butene not only undergoes reversible bond isomerisation to cis-2- and trans-2-butene and skeletal isomerisation to isobutene, but also, via butene dimerisation and cracking, oligomerisation, cracking and hydrogenation / dehydrogenation reactions. The extent of by-product formation can be limited by the choice of catalyst and operating conditions. (See also Appendix 1 for details of the definitions used and Section 2.3.3. for a review of the related literature) During the bench scale reactor study, using pure 1-butene and water as feed, some by-products were formed. The by-products partial pressure in the product gas was found to be less then 1.3 % of the system pressure. In comparison, the average n-butene, isobutene and water partial pressures in the flue gas were 25.3 %, 7.2 % and 66.2 % of the system pressure, respectively. A similar increase in the by-product partial pressure was observed across the pilot plant reactor system. Hence, as in both cases the increase in the by-products was not significant, all lighter (C_1 to C_3), heavier (C_5^+) and hydrogenated (n-butane and isobutane) by-products were treated as a single pseudo-component with average molecular weight equal to that of butene.

5.7 HOMOGENEOUS REACTION ACTIVITY

To ensure that the results obtained during the experimental investigations were due to the catalyst and not the preheat, reactor material nor homogeneous reactions, a series of blank tube experiments were conducted. As discussed in detail in Chapter 3, Section 3.2.5, it was found that homogeneous reactions were absent and that the packing material and the reactor system were inert. All results obtained from this system may therefore be attributed to the catalyst.

5.8 SYSTEM CONSTRAINTS AND ASSUMPTIONS

In view of the results and discussions presented above, the following conclusions may be reached regarding the complexity of the model required and the suitability of the reactor systems, both the pilot plant and the bench scale reactor system, for performing kinetic investigations.

- Deviations from ideal plug flow due to radial or axial mass transfer limitations were found not to be significant.
- Deviations from ideal plug flow due to radial or axial heat transfer limitations were found not to be significant.
- The resistance to inter - particle heat transfer was found not to be significant.
- Resistance to inter-particle mass transfer was found not to be significant at linear velocities in excess of 200 m/h.
- The resistance to intra - particle heat transfer was quantified and found not to be significant.
- Resistance to intra-particle mass transfer was found not to be significant irrespective of the size of catalyst particle used. The full size particle as supplied, with an average diameter of 1.5 mm, will be used during the kinetic investigation.
- The superficial linear fluid velocity was found to be independent of the bed height as pressure drop and molar volume expansion and / or contractions were absent.

Hence, heterogeneous models to describe both heat and mass transfer effects in and around the catalyst particle are not required while a simplified, one-dimensional pseudo-homogeneous reactor model may be used to model both the bench scale and pilot plant reactor systems. For component i,

$$-u \cdot \frac{\partial C_i}{\partial z} = r_i \cdot \rho_B \qquad 5\text{-}1$$

and boundary conditions at $z = 0$ of $C_i = C_{i,in}$ and $\partial C_i/\partial z = 0$ at $z = L$.

where

u is the superficial velocity in the axial direction, $m \cdot s^{-1}$,
C_i is the concentration of component i at the reaction conditions, $mol \cdot m^{-3}$,
$C_{i,in}$ is the concentration of component i in the feed at the reaction conditions, $mol \cdot m^{-3}$,
ρ_B is the density of the catalyst in the bed, $kg \cdot m^{-3}$,
z is the height of the element, m,
r_i is the global rate of disappearance of component i per unit mass of catalyst, $mol \cdot s^{-1} \cdot kg^{-1}$ and
L is the total bed length, m.

Furthermore,

- the reactor system and preheat material were inert,
- homogeneous reactions were absent,
- the linear butenes could be treated as a single pseudo-component, n-butene,
- the by-products could be treated as a single pseudo-component and
- only results for which the iso-butene to n-butene ratio in the product gas was less then 75 % of the theoretical value predicted from thermodynamics, were used during the kinetic investigation.

5.9 COMPUTATIONAL PROCEDURE

The mass conservation equation of the one-dimensional, homogeneous reactor model (Equation 5.1) was written for one component only. However, in this and other complex reaction systems a continuity equation must be written for each component, resulting in a set of differential equations which have to be solved simultaneously. The set of differential equations were solved by difference calculus with the differential terms being approximated by the backward differences. This approach does not suffer from the mathematical stability problems associated with the forward difference method (Keyser, 1996:4-8).

Using a dedicated FORTRAN program, adapted from one previously developed by Keyser (1996), the optimum values of the unknown parameters for each of the kinetic rate equations considered (See Chapter 6 for details) were determined. A brief description of the computational approach is given below, with a full algorithm and the actual source codes and data files used given in Appendix 3. To allow discrimination between the various kinetic rate expressions, a number of statistical techniques were used.

5.9.1 CALCULATION SEQUENCE

As the mass balance was set up for each component, the reaction rate for each component needed to be calculated. In this study, the linear butenes were treated as a single pseudo-component, n-butene as were the by-products. Hence, the stoichiometry of the transformation of the n-butenes to isobutenes could be represented by

$$\text{n - butene} \rightleftharpoons \text{isobutene} \qquad 5\text{-}2$$

and the transformation of the n-butenes to the by-products, i.e., losses, could be represented by

$$\text{n - butene} \rightarrow \text{by - products} \qquad 5\text{-}3$$

After having selected a n-butene skeletal isomerisation ($r_{Isomerisation}$) and a by-product (r_{Losses}) rate equation, as discussed in Chapter 6 and Appendix 3, the individual reaction rates for the various components were calculated from the reaction stoichiometry. For the formation of the by-products using

$$r_{By-Products} = + r_{Losses} \qquad 5\text{-}4$$

and for the butenes using

$$r_{n-C_4^=} = - r_{Isomerisation} - r_{Losses} \qquad 5\text{-}5$$

and

$$r_{i-C_4^=} = + r_{Isomerisation} \qquad 5\text{-}6$$

Using the outlet concentration from the previous reactor bed increment as both the inlet and outlet concentration of the subsequent element, the reaction rate, using the rate equations under consideration, was calculated for each reaction and so for each component. These rates were in turn used to calculate, together with the superficial velocity, increment height and catalyst bulk density, i.e., via the mass conservation equation of the one-dimensional reactor model, the new outlet concentration for each component. The new and old bed increment outlet concentration were compared, and if markedly different, the outlet concentration of each component was set to the new calculated outlet concentration, and the procedure repeated. If the difference was negligible, the next bed increment was considered. This procedure was repeated until the end of the catalyst bed was reached after which, using the final bed increment outlet concentration, the partial pressures of the various components in the flue gas were calculated as well as the deviation from the actual experimental values. This procedure was repeated for each experiment finally resulting in a global error, caused by the values selected for the constants associated with the rate equations under consideration. This error was in turn minimised by adjusting these variables, using the Levenberg-Marquardt procedure, and repeating the entire process. In this way the overall error obtained between the actual and calculated performance, for each of the rate equations under consideration, could be determined and using various statistical procedures, the rate equations ranked.

5.10 MODEL DISCRIMINATION

Using the derived rate equation, the performance of the system may be calculated. Using the calculated and experimental data, discrimination between rival rate equations is then possible via standard statistical procedures. Rival models may be discarded and the model with the best fit identified. The various statistical and error determination procedures used are discussed here.

5.10.1 ERROR DETERMINATION

Using the FORTRAN code set up together with the IMSL Levenberg-Marquardt routine, the optimum values of the unknown variables for each of the kinetic rate equations were determined. The error function minimised in each case was

$$err = \sum_{i=1}^{m} \left(\left(\frac{| p_{n-C_4}^{c_i} - p_{n-C_4}^{a_i} |}{p_{n-C_4}^{a_i}} \right)^2 + \left(\frac{| p_{i-C_4}^{c_i} - p_{i-C_4}^{a_i} |}{p_{i-C_4}^{a_i}} \right)^2 \right) \qquad 5\text{-}7$$

where

$p^a_{n\text{-}C4}$ is the actual n-butene partial pressure in the product gas, kPa(a),
$p^a_{i\text{-}C4}$ is the actual isobutene partial pressure in the product gas, kPa(a),
$p^c_{n\text{-}C4}$ is the calculated n-butene partial pressure in the product gas, kPa(a),
$p^c_{i\text{-}C4}$ is the calculated isobutene partial pressure in the product gas, kPa(a),
i is the experiment being considered, -,
m is the total number of experiments considered, - and
err is the overall sum of errors, -.

5.10.2 LACK OF FIT

A statistical F-test can be used to discriminate between rival rate equations. For a model to fit adequately, the following statistical relationship (Sarup and Wojchiehowski, 1989:70) has to be satisfied.

$$R = \frac{(SSQ - \delta^2 \cdot m) / (n - p - m)}{\delta^2} < F(n - p - m, m) \qquad 5\text{-}8$$

where

SSQ	is the sum of the residual squared at the optimum solution, -,
δ^2	is the pure error variance calculated from repeat data collected at the same reaction conditions, -,
m	is the number of degrees of freedom associated with the pure error variance, -,
n	is the number of experimental points, -,
p	is the number of parameters being estimated, - and
F(n-p-m,m)	is the tabulated F-test values, -, (Draper and Smith, 1981:533).

5.10.3 ANALYSIS OF RESIDUALS

The model fits were tested for lack of fit by a graphic inspection of the residuals plotted as a function of the calculated n-butene, isobutene and by-product partial pressures and mole fractions, the time on line, the n-butene and water feed rates, the catalyst mass, the system pressure and the system temperature. In all cases no structure in the residuals, which would be indicative of a lack of fit, could be identified (Draper and Smith, 1981).

5.10.4 COEFFICIENT OF DETERMINATION

The degree of fit between the actual and the calculated experimental data can also be quantified by calculating the coefficient of determination. The closer the coefficient is to one, the better the fit. The coefficient of determination may be calculated using

$$R^2 = 1 - \frac{\sum_{i=1}^{m} (Y_{A_i} - Y_{P_i})^2}{\sum_{i=1}^{m} (Y_{A_i} - \bar{y})^2} \qquad 5\text{-}9$$

where

R^2 is the coefficient of determination, -,

Y_{Ai} is the actual value for experiment i, -,

Y_{Pi} is the predicted value for experiment i, -,

$\bar{y}$ is the average of the actual values, -,

m is the number of experiments, - and

i is the experiment number -,.

5.10.5 CONFIDENCE INTERVALS

The confidence intervals for parameters determined by non linear regression were calculated from confidence contours (Draper and Smith, 1981). These confidence intervals are however only exact if the models are linear or if a linearised form of a non-linear model is used. In the case of this study, the models are non-linear and therefore the confidence intervals are not exact, and should be regarded as approximate confidence intervals only. The confidence contour is given by

$$\frac{err}{err'} = 1 + \frac{p}{n - p - m} \cdot F(n - p - m, m) \qquad 5\text{-}10$$

where

err is the sum of errors at the optimum solution, - and

err' is the sum of errors away from the optimum solution, -.

With the value of err known at the optimum solution, the value of err' some distance away from the optimum solution, can be calculated from Equation 5.10. The value of each particular parameter was then varied until the value of err which was obtained from the model output equalled the value of err' as calculated from Equation 5.10. Logically, the optimum value of each parameter had to be varied above and below its optimum value in order to obtain the interval around the optimum value. All confidence intervals were calculated with tabulated F-values at 95% significance levels.

5.10.6 MAPPING OF CONFIDENCE CONTOURS

In performing the non-linear regression procedures, some of the rate constants could not be determined uniquely. For a different set of starting conditions a different set of rate constants was obtained as the optimum solution. In an attempt to overcome the short comings of the confidence interval analysis, a parameter sensitivity analysis was performed on each of the rate constants. This entailed mapping the error (err) against the value of each of the variable parameters while the values of the other parameters were maintained at the optimum values.

Briefly, three basic types of confidence contours for the pre-exponential factors and activation energies were obtained. Stylised examples of these are shown in Figures 5.7 to 5.9. The following conclusions may be drawn from these contours. A symmetrical confidence contour about the optimum value for both the activation energy and the pre-

exponential factor, as shown in Figure 5.7, will be obtained when a single solution exists. A confidence contour of this type suggests that the error is very sensitive to the rate of the reaction step under consideration, i.e., that the rate of this reaction step is critical.

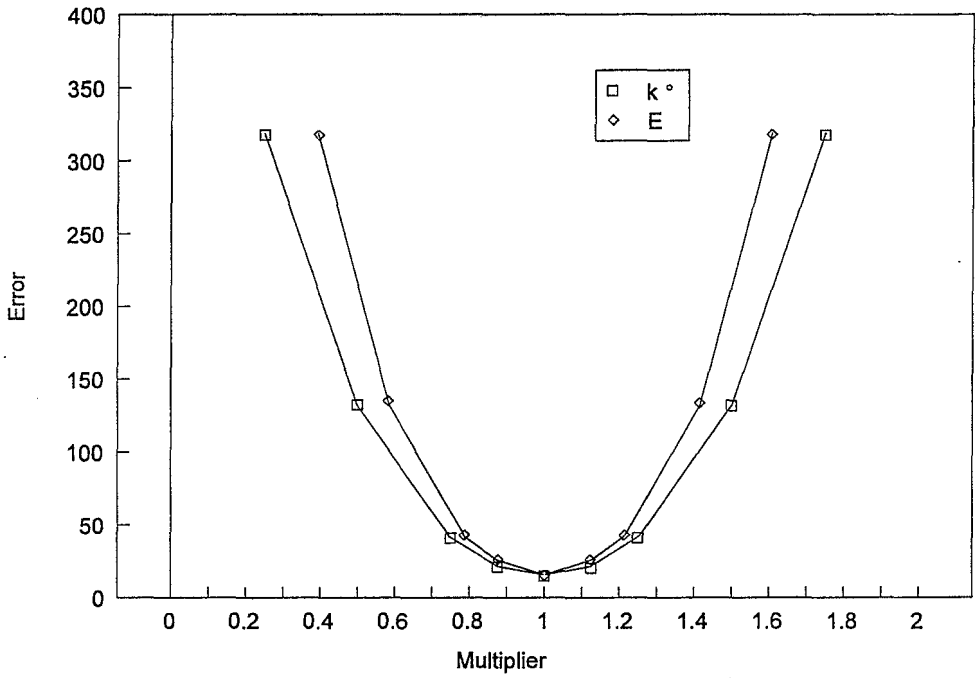

Figure 5.7 : Contour plot obtained for a defined reaction rate

Alternatively, a combination of confidence contours as shown in Figures 5.8 or 5.9 may be obtained. With all else being held constant, increasing the value of the pre-exponential factor will result in a increase in the reaction rate, while increasing the absolute value of the activation energy, will result in decrease in the reaction rate. Hence, these combination of contours suggest that the reaction rate under consideration must either be greater than some limiting value (Figure 5.8) or smaller than some limiting value (Figure 5.9) to minimise the error. A critical examination of the confidence contours obtained for each of the mechanistic models considered, is presented in Chapter 6.

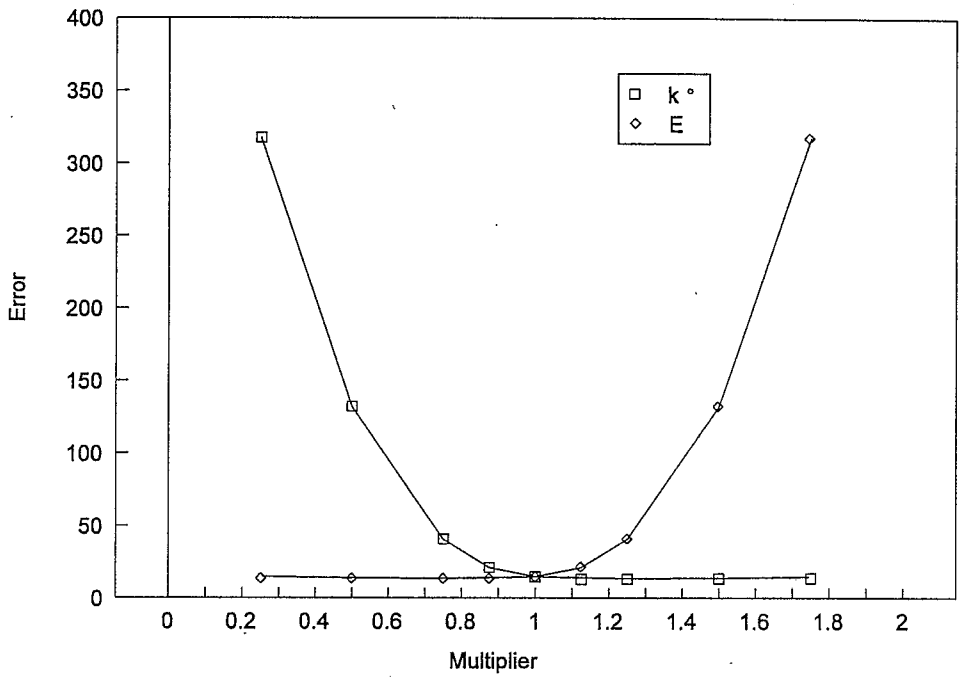

Figure 5.8 : Contour plot obtained if the rate must be larger than some limiting value

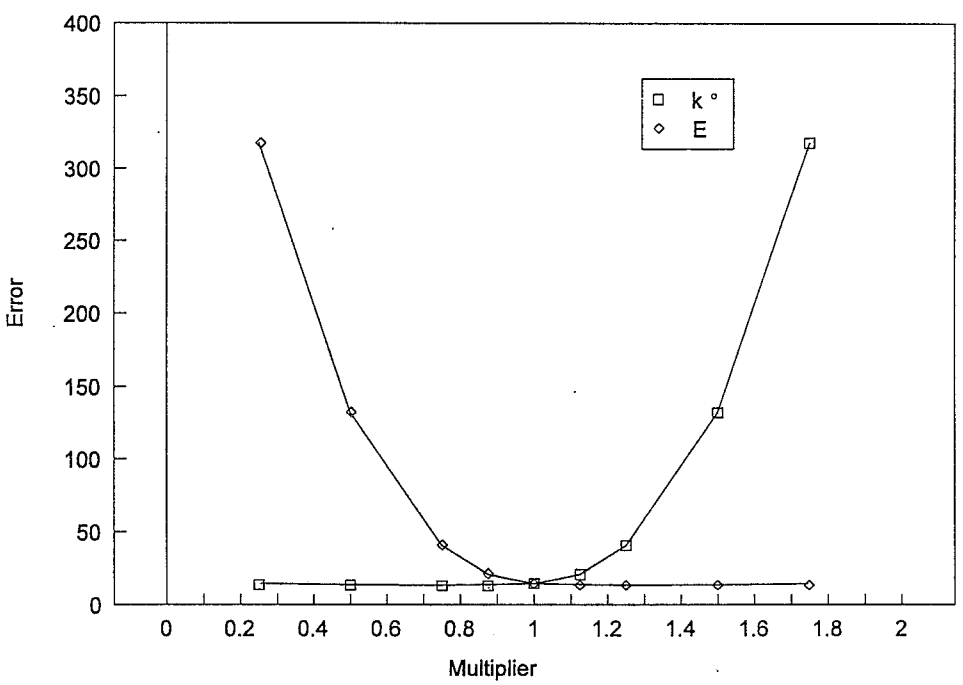

Figure 5.9 : Contour plot obtained if the rate must be smaller than some limiting value

5.10.7 CONFIRMATION OF PROCEDURE

The capability of the procedures developed to distinguishing between the rival models was investigated. Using the optimum values of the unknown parameters determined for Case 8, a fictitious set of "measured" responses at each of the 392 sets of operating conditions, was generated. Next, using these "measured" responses, the error obtained when fitting each of the other seven cases under consideration to the data, was determined. The results obtained are shown in Table 5.6 below.

TABLE 5.6 : ERROR WHILE FITTING DATA GENERATED USING CASE 8

Case	err	Case	err
Case 1	0.3030	Case 5	0.0843
Case 2	0.0232	Case 6	0.0220
Case 3	0.0324	Case 7	0.0241
Case 4	0.1089	Case 8	0.0001

As may be seen from this table, it was not possible to fit the rival models to the "measured" data. In each case the error obtained was more than two orders of magnitude greater than that recorded when refitting Case 8 to the fictitious data set. The ability of the procedures developed to discriminate between rival models was therefore confirmed.

5.11 KINETIC STUDY - EXPERIMENTAL REGIONS

The kinetic data was generated using the bench scale reactor system by simultaneously varying one or more of the operating parameters. The limits between which the parameters were adjusted are shown in Table 5.6 and Figure 5.10 below.

TABLE 5.7 : EXPERIMENTAL REGION - KINETIC STUDY

Parameter	Bench Unit			Pilot Unit		
	Minimum	Average	Maximum	Minimum	Average	Maximum
Temperature, °C	406.7	526.3	569.6	470.9	516.4	544.9
Pressure, kPa(a)	85.0	152.6	215.0	85.0	146.2	205.7
Water / Butene, mole ratio	0.94	2.06	6.06	1.35	1.95	3.31
Butene WHSV, h^{-1}	0.53	2.03	5.94	0.65	1.82	1.95

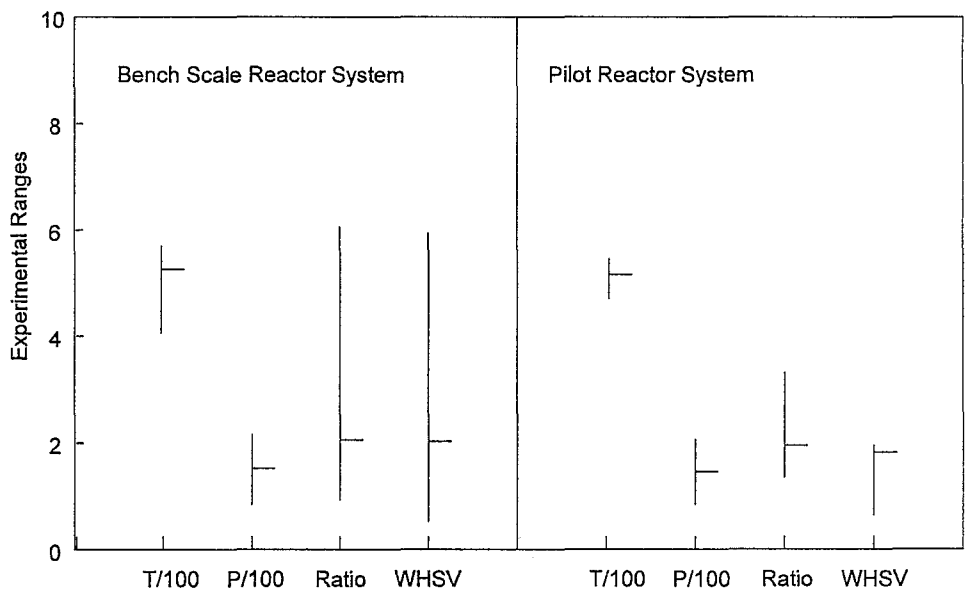

Figure 5.10 : Bench scale and pilot plant reactor systems experimental ranges

5.12 SUMMARY

The kinetics of this reaction were investigated in an attempt to identify the reaction mechanism and to develop the intrinsic kinetic equation. The necessary experimental data was generated using the bench scale reactor system. Of course, prior to performing a kinetic study, the suitability of the experimental equipment and the complexity of the reactor model required had to be established. Using various theoretical techniques as discussed, by among others, Smith (1981:557), Mears (1971:544), Froment and Bischoff

(1979:451) and Carberry (1981:76), the significance of both radial and axial heat and mass transfer limitations were quantified. It was concluded that the flow patterns in both the pilot plant and the bench reactor system did not deviate sufficiently from ideal plug flow to warrant the use of a two-dimensional reactor model. Also, from a theoretical as well as experimental investigation, using the techniques proposed, by among others, Mears (1971:128), Everson et al. (1996:238) and Froment and Bischoff (1990:173), it was concluded that mass and heat transfer limitations in and around the catalyst particle were not significant. Hence, it was concluded that a one-dimensional pseudo-homogeneous reactor model may be used to describe the reactor system, while heterogeneous models to describe heat and mass transfer effects in and around the particle, were not required. Furthermore, all results recorded were due to the catalyst, as homogeneous gas phase reactions did not take place and the reactor and packing material were inert. Finally, as the reactor systems were operated isothermally, in both the axial and the radial direction, isobarically in the axial direction, and as the molar flow rate remained constant throughout, the superficial linear velocity in both the pilot plant reactor system and the bench scale reactor systems were independent of the axial position in the catalyst bed, allowing further simplification of the reactor model.

It is, of course, not possible to investigate the kinetics of a system in which the composition of the products is independent of the operating conditions, as is the case if the products are at thermodynamic equilibrium. During the kinetic investigation only results for which the iso-butene to n-butene ratio in the product gas was less then 75 % of the theoretical value predicted from thermodynamics. The thermodynamic equilibrium composition of the butenes as a function of temperature was obtained from the literature (Kilpatric et al., 1946:559) and calculated using two process engineering modelling packages, Proll and AspenPlus. The influence of the thermodynamic equilibrium on the suitability of the data for kinetic studies was not previously reported in the literature.

The molar ratios of the linear butenes, on the other hand, were independent of the operating conditions. In all cases the recorded ratios were as predicted from thermodynamics. This permitted that the linear butenes, 1-butene, cis-2-butene and trans-2-butene could be treated as a pseudo-component, n-butene during the kinetic study.

Similarly, the by-products, formed via the disproportionation of the butenes (Andy et al., 1998:322) were treated as a single pseudo-component as was previously done by Choudhary and Doraiswamy (1975:228). The rate equations required, based on the mono-molecular mechanism (Choudhary and Doraiswamy, 1975:235) when a single step, or multiple steps, control the overall reaction rate were developed, as discussed in Chapter 6 and Appendix 3 (Froment and Bischoff, 1979:73). To fit the various rate equations to the experimental data, i.e., to identify the optimum values of the unknown parameters, the necessary FORTRAN program was set up. Attempting to model the n-butene skeletal isomerisation reaction using a multi-step approach, was not previously reported in the literature.

To allow discrimination between rival models, a number of statistical techniques (Sarup and Wojchiehowski, 1989:70, Draper and Smith, 1981:533, Box et al., 1978:43) were employed. Confidence intervals and confidence contours, about the optimum values of the unknown parameters required by the various rate equations, were also generated. The use of confidence contours to confirm that the optimum value of the unknown parameters was indeed located in each case was not previously reported for this system in the literature. Using a fictitious data set, the ability of the procedures developed to discriminate between rival models was also confirmed.